TOOLS AND RESOURCES

In situ imaging of mitochondrial translation shows weak correlation with nucleoid DNA intensity and no suppression during mitosis

Christopher Estell[1], Emmanouela Stamatidou[2], Sarah El-Messeiry[2,3] and Andrew Hamilton[2,*]

ABSTRACT

Although mitochondrial translation produces only 13 proteins, we show here how this process can be visualised and detected *in situ* by fluorescence microscopy with a simple, rapid and inexpensive procedure using non-canonical amino acid labelling and click chemistry. This allows visualisation of the translational output in different mitochondria within a cell, their position within that cell and a comparison of mitochondrial translation between cells. The most highly translationally active mitochondria were closest to the nucleus but were also found at the distal end of long cellular projections. There were substantial differences in translation between adjacent mitochondria and this did not readily correlate with apparent mitochondrial genome content. Mitochondrial translation was unchanged during mitosis when cytoplasmic translation was suppressed. This method will serve both fundamental cell biology and clinically orientated studies, in which mitochondrial function is a key parameter.

KEY WORDS: Mitochondria, Translation, Labelling, Fluorescence, Click

INTRODUCTION

Mitochondria are unique among animal organelles in that they possess their own genome that encodes only 13 proteins (Gustafsson et al., 2016) in contrast to >1000 mitochondrial proteins encoded by the nuclear genome (Pagliarini et al., 2008). Despite their relatively small number, mitochondrion-encoded proteins are essential components of the oxidative phosphorylation pathway, and mitochondrial genome mutations are strongly linked to ageing and degenerative diseases (Park and Larsson, 2011). The number of mitochondria per cell is in the order of several hundred, but this changes continuously due to fission and fusion of these organelles (Westermann, 2010). Mitochondrial DNA is packaged in structures called nucleoids, which usually contain one or two copies of the mitochondrial genome; however higher copy number nucleoids exist (Kukat et al., 2011; Bogenhagen, 2012; Gustafsson et al., 2016) and, again due to fission/fusion, the exact number of nucleoids per organelle must vary continuously. Gene amplification is a common mechanism for increasing expression—plasmids and oncogenes being obvious examples—and it is reasonable to propose that increased mitochondrial DNA content per nucleoid or per organelle results in increased protein synthesis. However, this has

not been tested because no method exists to examine total mitochondrial genome and *de novo* expression simultaneously *in situ*. Mitochondrial genome polymorphisms (heteroplasmy) is also common in mammalian cells (Larsson, 2010; He et al., 2010), partly due to the much higher mutation rate of mitochondrial DNA compared to nuclear DNA (Taylor et al., 2003) but, again, it is not known how such sequence variation affects overall genome expression. Heterogeneity of mitochondrial membrane potential and activity of some mitochondrial enzymes have been observed and associated with disease (Wikstrom et al., 2009), in a way similar to that of genetic polymorphism. However, the extent to which such physiological heterogeneity arises from mitochondrial gene variability is, again, unknown partly due to the paucity of methods for imaging global mitochondrial gene expression.

Methods to image protein expression within mitochondria are limited to traditional immunofluorescence analyses of individual proteins. However, these show only the steady-state level of the protein studied and do not reveal any dynamic changes or reveal rates of overall translation. Global synthesis of new mitochondrion-encoded proteins has been studied by either using radioactively (^{35}S)-labelled methionine (Met) (Sasarman and Shoubridge, 2012; Gao et al., 2016), or non-canonical amino acid analogues of Met (Zhang et al., 2014). Both procedures used either polyacrylamide gel electrophoresis (PAGE) or mass spectrometry (MS) analyses of protein extracts and therefore did not detect inter-mitochondrion variations or the spatial distribution of translationally active mitochondria within the cells. Non-canonical amino acid labelling can also be used for *in situ* imaging of total cytoplasmic protein synthesis because the incorporated amino acid analogues can be coupled to fluorescent reporter molecules after labelling through chemo-selective, bio-orthogonal 'click' reactions. This allows detection only of proteins synthesised during the labelling period by fluorescence microscopy, i.e. without interference from pre-existing proteins (Dieterich et al., 2006; Beatty et al., 2006; Beatty, 2011). However, the sensitivity of these methods, apparently, did not extend beyond detection of total cytoplasmic protein synthesis that, of course, constitutes the vast majority of translational cellular output. In these reports, confirmation that labelling was the result of translation was demonstrated by the absence of detectable labelling in the presence of cycloheximide (CHI), a potent inhibitor of cytoplasmic translation. Translation of the mitochondrial genome (hereafter referred to as Mt translation) – which is insensitive to CHI – was not detected in these experiments, although it is known to incorporate these non-canonical amino acids (Zhang et al., 2014). It is likely that, since translation of the mitochondrial genome produces only 13 proteins, labelling of these proteins was below the threshold of detection available with the procedures employed. Here, we describe how labelling cells with a non-canonical amino acid followed by click reaction with a fluorescent azide can, in fact, be used to observe global Mt translation *in situ* by epi-fluorescence microscopy. We show how the background fluorescence, which

[1]Institute of Cancer Science, Glasgow University, Glasgow G61 1QH, UK.
[2]School of Medicine, Dentistry and Nursing, Glasgow University, Glasgow G12 8QQ, UK. [3]Department of Genetics, Faculty of Agriculture, Alexandria University, Alexandria, Egypt.

*Author for correspondence (andrew.hamilton@glasgow.ac.uk)

C.E., 0000-0002-2820-2961; E.S., 0000-0001-5937-3280; S.E., 0000-0002-3115-5625; A.H., 0000-0002-1269-5423

would otherwise obstruct detection of Mt translation, can be eliminated by simple adjustment of the cell fixation procedure. This method reveals the spatial heterogeneity of the output of Mt translation within a cell and its consistency through mitosis, and our findings demonstrate the utility of our method for both fundamental and clinically orientated studies of mitochondrial gene expression.

RESULTS

Cell permeabilisation before cell fixation greatly reduces background fluorescence after labelling with HPG

In the first report of *in situ* imaging of protein synthesis that used the 'clickable' Met analogue homopropargylglycine (HPG), genuine incorporation by cytoplasmic translation in mouse embryonic fibroblasts was confirmed by eliminating the detectable signal with CHI (Beatty et al., 2006). Following a similar labelling and fixation procedure, we observed similar HPG incorporation into cells of the mouse C2C12 cell line (Fig. 1Ai) that was also strongly suppressed in the presence of CHI (Fig. 1Aii). Suppression of cytoplasmic translation by CHI should have revealed any underlying Mt translation. However, our attempts to observe this by extending the fluorescence exposure time of HPG+CHI-treated cells were confounded by excessive background fluorescence (Fig. 1Bii). This background signal was undiminished by high concentrations of puromycin (Fig. 1Biii), which should inhibit all HPG incorporation by protein synthesis, but was absent from cells that had not received HPG treatment (Fig. 1Bi), suggesting that it originated from trapped HPG reacting with fluorescent azide. We had followed the procedure

of Beatty et al. (2006) that employed a widely used formaldehyde-based cell fixation procedure followed by permeabilising cells with detergent. Therefore, we investigated whether brief permeabilisation of cells before fixation with digitonin, a detergent exerting minimal effect on mitochondria, allows the escape of free HPG and, thus, a reduction of background signal. This simple modification all but eliminated the background fluorescence, leaving a fainter but clearly visible punctate/rod-like pattern (compare Fig. 1Bii with Cii) that was stronger and distinct from the trace fluorescence in control cells not treated with HPG (compare Fig. 1Cii and Ci).

CHI-resistant HPG labelling is qualitatively different to HPG labelling without CHI

It is possible that the pattern of fluorescence observed in CHI-treated cells that had been made permeable before fixation (Fig. 1Cii) was simply due to incomplete inhibition of cytoplasmic translation by CHI i.e. a weak version of HPG-only labelling. Therefore, we compared the total cytoplasmic translation and putative mitochondrial translation by using the optimised permeabilisation and fixation procedure (Fig. 2). Without CHI there was rapid synthesis and nuclear import of nucleolar proteins that made up a substantial proportion of newly synthesised protein in total. Also, we observed distribution of new proteins throughout the cytoplasm (Fig. 2Ai). In contrast, in the presence of CHI (Fig. 2Bi), no nucleolar signal could be detected and the cytoplasmic signal was punctate or rod-like rather than diffuse. Although long exposure times were necessary to detect any signals, their strength was still 20−200 times
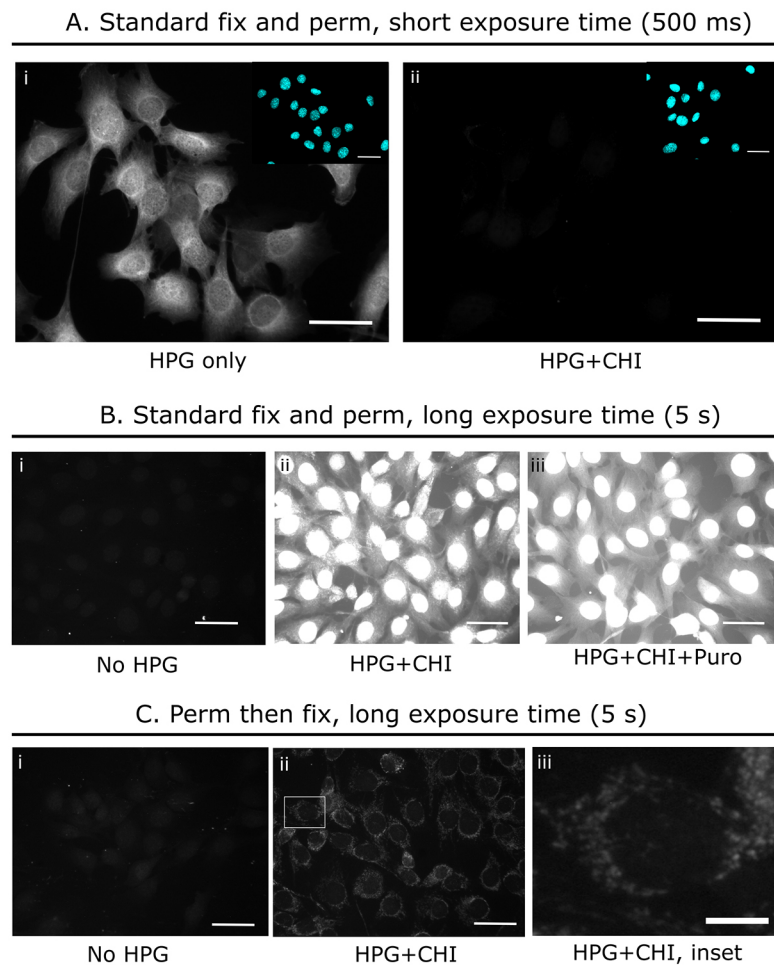
A. Standard fix and perm, short exposure time (500 ms)

HPG only   HPG+CHI

B. Standard fix and perm, long exposure time (5 s)

No HPG   HPG+CHI   HPG+CHI+Puro

C. Perm then fix, long exposure time (5 s)

No HPG   HPG+CHI   HPG+CHI, inset

Fig. 1. Background fluorescence observed from trapped HPG under standard conditions are removed following pre-fix permeabilisation. C2C12 cells were incubated for 10 min with HPG, with our without inhibitors (annotated); proteins with incorporated HPG were labelled with fluorescent azide in a click reaction, and imaged by epifluorescence microscopy. Standard conditions: 10 min formaldehyde fix followed by a 10 min post-fix permeabilisation using 0.1% Triton X-100. (A) Exposure time of 500 ms (DAPI staining in inset) under standard conditions. (B) Exposure times of 5 s were used for cells not treated with HPG (i), and cells treated with CHI (ii) or CHI and puromycin (iii) under standard conditions. (C) Optimised conditions employ a 2 min pre-fix permeabilisation using 0.015% digitonin on ice followed by a 10 min formaldehyde fix and exposure time of 5 s. Images within the same set (1 A,B or C) have the same exposure times and are displayed with identical brightness and contrast settings. Scale bars: 50 μm (Ai, ii; Bi, ii, iii; Ci, ii) and 10 μm (Cii, magnified inset in Cii).
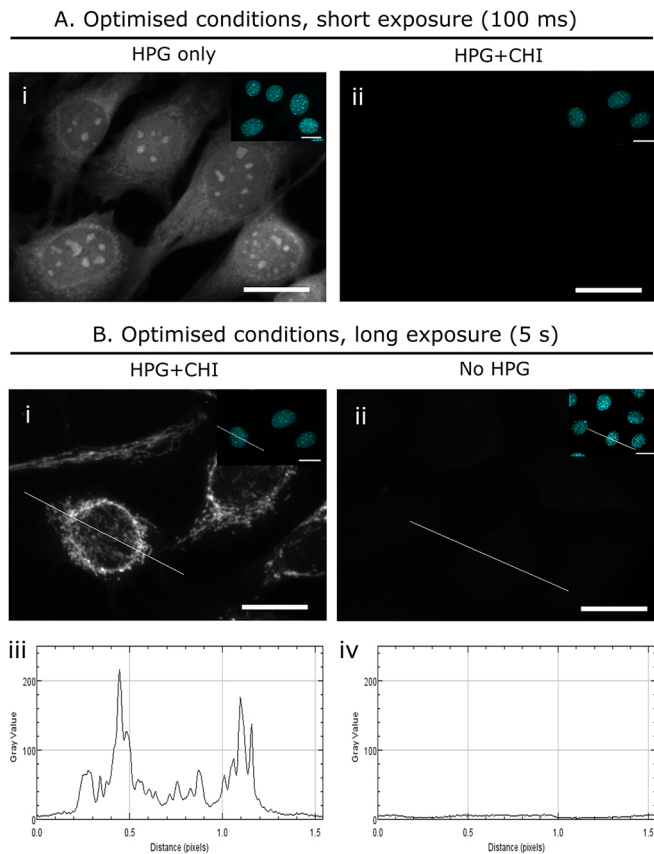
Fig. 2. Qualitative assessment of protein synthesis in HPG-treated C2C12 cells with or without CHI under optimised conditions. (A,B) C2C12 cells were incubated for 10 min with HPG and with or without CHI, permeabilised on ice with 0.015% digitonin for 2 min, and fixed with formaldehyde for 10 min. Proteins with incorporated HPG were labelled with fluorescent azide in a click reaction, and imaged by epifluorescence microscopy after exposure times of 100 ms (A) or 5 s (B). HPG-negative controls were exposed to the same click reaction with fluorophore to control for non-specific reactions or adsorbance. Relative fluorescence intensities along the white lines that traverse a cell incubated with HPG+CHI or without HPG were calculated by using the 'plot profile' tool in ImageJ (Biii, iv). Insets show DAPI staining of the same cells. Images with same exposure times are displayed with identical brightness and contrast settings. Scale bars: 20 µm.

higher than background fluorescence levels (Fig. 2Biii,iv). Essentially the same differential (HPG versus HPG+CHI) labelling patterns were observed in mouse (Eph4) and human (MCF-7) mammary epithelial cells (Figs S1 and S2).

CHI-resistant in situ labelling with HPG is the result of mitochondrial protein synthesis

If the HPG+CHI signal truly represents mitochondrial translation it should be resistant to other antibiotics that selectively inhibit cytoplasmic translation, irrespective of their mechanism or the stage of translation they affect. Fig. 3ii shows that Harringtonine – that is, like CHI, an elongation inhibitor – allowed HPG incorporation in the same pattern as in response to treatment with CHI (Fig. 3i). Pactamycin, which inhibits cytoplasmic translation initiation, also generated this pattern, indicating that it is not due to HPG-labelled nascent proteins arrested on stalled polyribosomes (Fig. 3iii). Puromycin, which inhibits both translation in cytoplasm and mitochondria (but not the activity of amino acyl transferases) (Pestka, 1971), eliminated the signal, confirming it was due to genuine protein synthesis and not residual unincorporated HPG

retained within the fixed cells or HPG-charged tRNA (Fig. 3iv). Chloramphenicol (CAP), which specifically inhibits Mt translation in eukaryotic cells (Sasarman and Shoubridge, 2012), combined with CHI also eliminated the signal (Fig. 3v). Together, these results strongly suggested the CHI-resistant signal was due to Mt translation.

CHI-resistant HPG labelling colocalises with proteins expressed in mitochondria, mitochondrial 12S rRNA and nucleoid DNA but shows unexpected heterogeneity

Products of de novo Mt translation should colocalise with specific mitochondrial proteins detected by immunofluorescence. Fig. 4i-iii shows the HPC+CHI signal strongly colocalising with the mitochondrion-encoded cytochrome oxidase 1 (MT-CO1) protein (mean Pearson correlation coefficient of 0.9). There was some discrepancy – particularly at the distal end of the long cytoplasmic projections that are often observed in cells of the C2C12 cell line – in intensity between the two signals, which is likely to reflect the prolonged stability of MT-CO1 in mitochondria that have become less translationally active. This illustrates the differences observed when imaging steady-state protein levels by immunofluorescence instead of using more dynamic methods, such as ours.

The HPG+CHI signal also broadly colocalised with mitochondrial 12S rRNA (Fig. 4iv-vi) detected by fluorescence in situ hybridisation (FISH) and with nucleoid DNA detected by DAPI (Fig. 4vii-ix). However, closer examination of Mt translation versus either mitochondrial 12S rRNA or nucleoid DNA often revealed a lack of correlation of intensity: regions of higher DAPI or 12S rRNA intensity were often not adjacent to regions of higher translation activity. Similarly, clear translational activity was often found adjacent to weak or barely visible DAPI staining or 12S rRNA. This lack of correlation was more apparent in MCF-7 cells (Fig. 5A), which often contained several areas along the mitochondrial network that were strongly stained by DAPI (as revealed by translation imaging; Fig. 5Aiv) and were clearly not sites of elevated translational activity. Signal intensity for HPG and DAPI were measured using ImageJ (Materials and Methods), plotted and a regression line was calculated (Fig. 5B). The low coefficient of determination (R^2=0.3458) supports the argument that there is no simple, positive and linear relationship between the amount of nucleoid DNA and translational activity. Note that the DNA signal was not due to Mycoplasma spp. infection, i.e. the cell lines tested negative for Mycoplasma spp. using a commercial test kit. Visualisation of Mycoplasma spp. DNA with DAPI does not require the extended exposure times (Uphoff et al., 1992) used here since the genome of Mycoplasma spp. is far larger than that of a mitochondrion. Furthermore, MT-CO1 colocalised with the punctate, cytoplasmic DAPI signal, confirming that the latter is mitochondrial nucleoid DNA (Fig. S3).

Mitochondrial translation is not suppressed during mitosis

In situ imaging of cultured cells by DAPI staining readily reveals any cells that are in mitosis. Translation on cytoplasmic ribosomes is generally thought to be strongly reduced during mitosis, although early studies have shown that the extent of suppression is highly dependent on the cell type studied (Prescott and Bender, 1962; Konrad, 1963). The suppression of protein synthesis during mitosis can be easily observed by combining DAPI staining and HPG incorporation. C2C12 cells showed little suppression of protein synthesis during mitosis, whereas strong suppression in Eph4 cells and moderate suppression in MCF-7 cells (Fig. 6A and Figs S1 and 2) was observed. When the same imaging technique was used in the

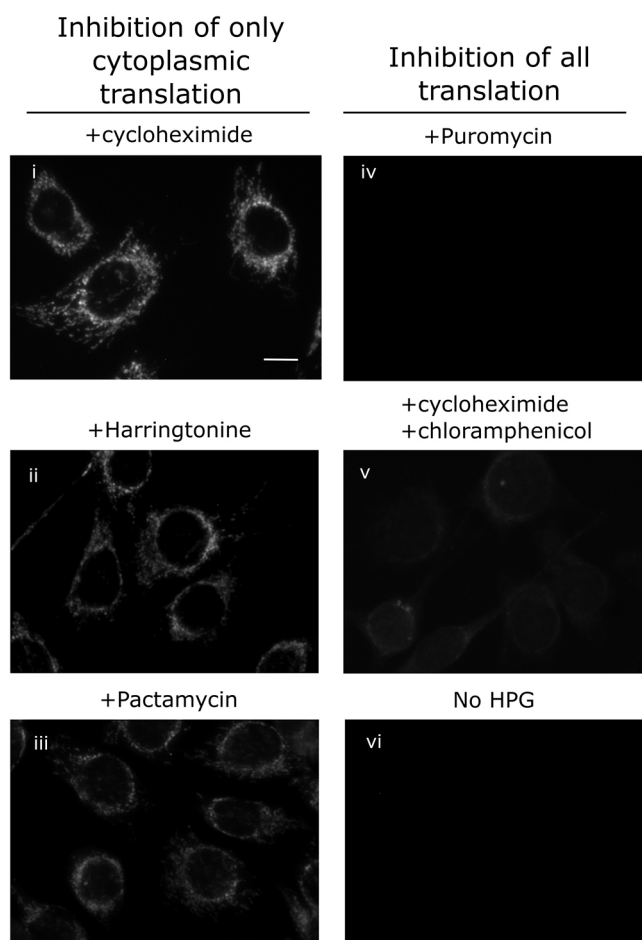## Inhibition of only cytoplasmic translation

Fig. 3. Consistent HPG incorporation pattern with different inhibitors of cytoplasmic translation; elimination with inhibition of all cellular protein synthesis. (i-vi) C2C12 cells were incubated with HPG and the translation inhibitors CHI (i), Harringtonine (ii), pactamycin (iii), puromycin (iv) or CHI plus chloramphenicol (v), or without HPG (vi). All click images were visualised for 5 s and displayed with the same brightness and contrast settings. Scale bar: 20 µm.

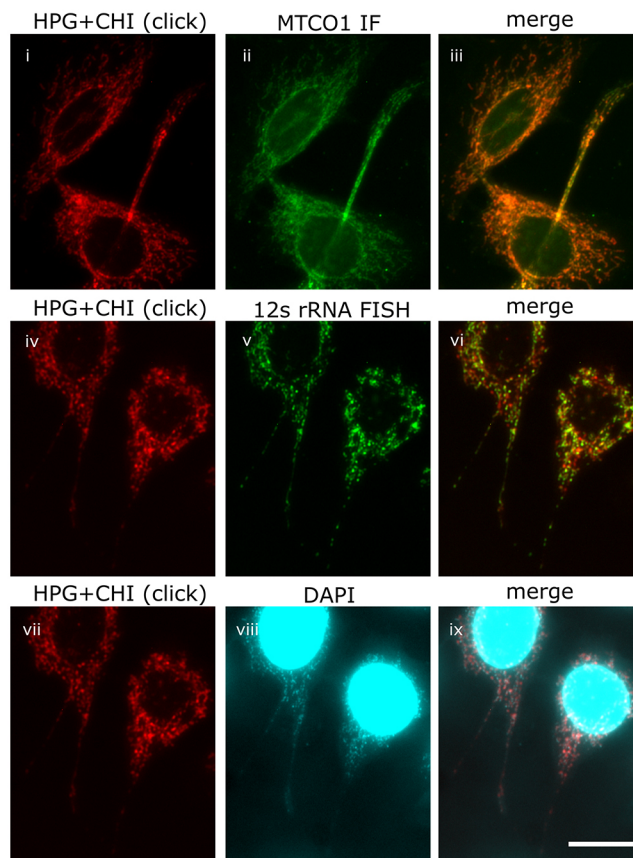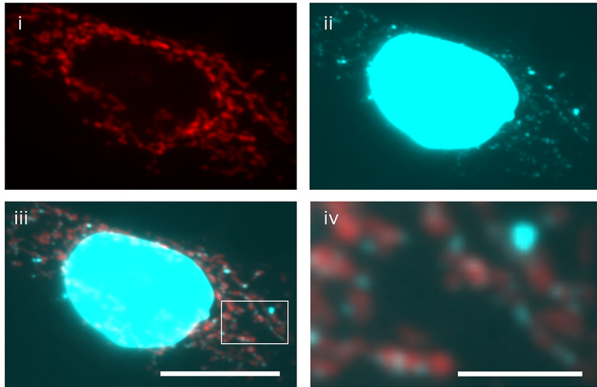## Colocalisation of mitochondrial translation with mitochondrial molecular markers

Fig. 4. Colocalisation of incorporated CHI-resistant HPG with MT-CO1, 12S rRNA and cytoplasmic DNA. C2C12 cells were labelled with HPG in the presence of CHI and translation was detected by click reaction with fluorescent azide (i, iv, vii). Subsequently, MT-CO1 protein (MTCO1) was detected by immunofluorescence (ii), 12S rRNA was detected by RNA FISH (v) and DNA by DAPI staining (viii). DAPI exposure was for 500 ms, ~50 times longer than normally used for nuclear DNA imaging. Merged images show colocalisation of these three molecular markers with mitochondrial translation (iii, vi, ix). Colocalisation of MT-CO1 and Mt translation was quantified using Image J with the COL2 plugin on 18 cells, giving a mean Pearson correlation coefficient of 0.90 (i.e. 90% colocalisation), ±s.d.=0.04. Scale bar: 20 µm.

presence of CHI to reveal mitochondrial translation, this was found to be unaffected in mitotic cells of any of the three cell lines (Fig. 6B).

DISCUSSION

We have developed a simple and rapid method of labelling *de novo* translation in mitochondria, which allows *in situ* imaging by epifluorescence microscopy (Figs 1 and 2). The key step is to permeabilise cells before fixation with a reagent (digitonin) that leaves mitochondria intact but allows release of any unincorporated labelling amino acid that otherwise becomes fixed and fluorescence labelled, thereby obscuring any genuine signal of mitochondrial protein synthesis. Mitochondrion labelling with the clickable amino acid analogue HPG was achieved by simultaneously inhibiting cytoplasmic translation within the cytoplasm in the presence of CHI. The response of this CHI-resistant HPG labelling to other antibiotics was entirely consistent with incorporation by mitochondrial ribosomes. Furthermore, we demonstrated that the *de novo* CHI-resistant HPG signal colocalised with mitochondrion-specific markers, such as MT-CO1, MT-DNA and MT-12S-rRNA (Fig. 4), detected by immunofluorescence, DAPI staining and FISH, respectively. These results also showed how our method can be easily combined with other commonly used methods in cell biology. It is also worth noting that our method does not require

extensive (0.5−4 h) pre-incubation of cells in Met-free medium, as described in other protein labelling protocols (Hodas et al., 2012; Beatty et al., 2006; Dieterich et al., 2006; Zhang et al., 2014), thereby mitigating concerns that artefactual translational programmes are established before labelling treatments (Goodman et al., 2012).

In the course of developing and testing the method we made two observations that exemplify the utility of our method, and might serve as primers for further, more-detailed, investigation. First was our observation that, although, the distribution of mitochondrial rRNA and DNA closely coincided with regions of translation, signal intensities correlated only infrequently. This was surprising, as one might reasonably suspect that mitochondrial genome amplification serves as a mechanism to boost mitochondrial protein expression and that ribosome content determines translational output. However, this was often not the case. Particularly in the cancer cell line MCF-7, we frequently observed mitochondria with DAPI fluorescence greatly exceeding that of other surrounding nucleoids. DAPI fluorescence of mitochondrial DNA correlates well with other methods used to estimate mitochondrial DNA, such as the use of anti-DNA antibodies

A. Mitochondrial translation in an MCF-7 cell

B. Distribution of translation intensity vs. DNA intensity
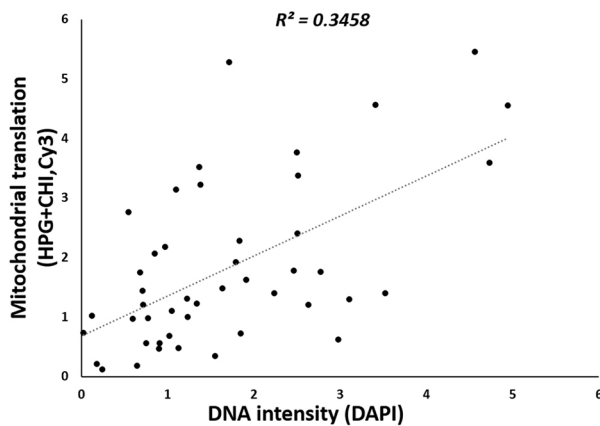

Fig. 5. Strength of mitochondrial translation does not correlate perfectly with the amount of mitochondrial DNA. (A) MCF-7 cells were labelled with HPG in the presence of CHI; mitochondrial translation was detected by click reaction with a fluorescent azide (i). Staining with DAPI and prolonged camera exposure allowed imaging of mitochondrial DNA as punctate spots and rods in the cytoplasm (ii). The merged image and magnified inset (iii, iv) show blue DAPI staining within or adjacent to the products of mitochondrial translation. Scale bars: 20 μm (i-iii), 5 μm (iv). (B) A total of 46 ROIs I from seven cells were created using ImageJ. Each ROI encompassed punctate cytoplasmic DAPI staining and surrounding fluorescence from adjacent mitochondrial translation. Mean red (translation) and blue (DNA) fluorescence was calculated for each ROI. Background fluorescence in both channels was calculated individually from each cell as the mean of at least four ROIs that lacked either punctate DAPI staining or rod-like red fluorescence, and was subtracted from values obtained from each mitochondrial region within that cell. These total corrected red and blue fluorescence values for each region were plotted, and a regression line and R^2 value were calculated using Microsoft Excel software.

(Kukat et al., 2011), indicating these mitochondria have greatly amplified genomes. However, they did not exhibit correspondingly higher translation (Fig. 5A) and it will be of interest to explore exactly how such suppression of the mitochondrial genome is achieved, and whether this is a response to other cellular failures or, rather, an instrumental stage in processes, such as apoptosis.

In situ methods, such as ours, also readily allow observation of events during mitosis, as this stage of the cell cycle can be easily identified by DAPI staining. Cytoplasmic translation is generally thought to be suppressed at this stage (Prescott and Bender, 1962); this was evident in Eph4 cells (Fig. S1i) and, to some extent, in Mcf-10a cells (Fig. S2i). Our method shows, for the first time, that Mt translation during mitosis is not similarly suppressed (Figs S1v,vi

De novo translation at mitosis
A. Total translation (HPG only)
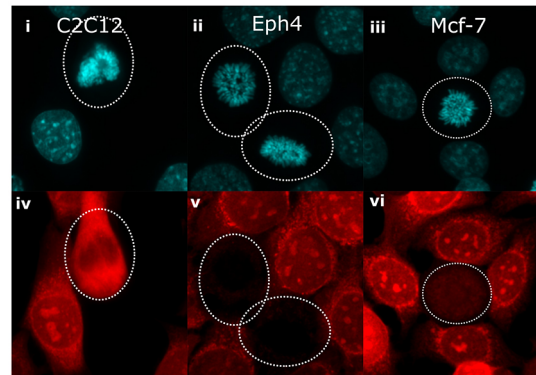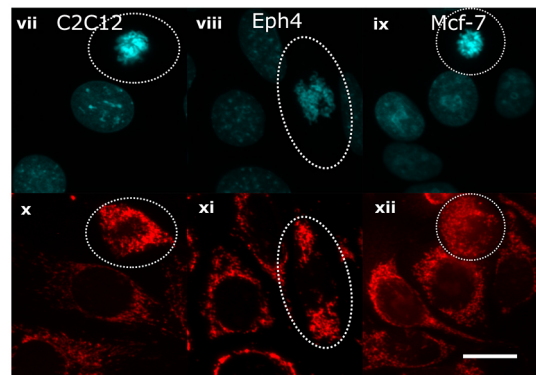

B. Mitochondrial translation (HPG+CHI)

Fig. 6. *De novo* translation at mitosis. (A,B) C2C12, Eph4 and MCF-7 cells were labelled with HPG alone (A) or HPG plus CHI (B) and DAPI stained (i-iii; vii-ix). Newly translated proteins were detected by click reaction with fluorescent azide (iv-vi; x-xii). Mitotic cells at pro-metaphase are encircled. Scale bar: 20 μm.

and 2iii,iv). This raises the question as to how cells would balance the assembly of protein complexes originating from two different genomes during this phase of the cell cycle. Such observations illustrate the advantages of our *in-situ* method for revealing unexpected results and generating new hypotheses to be tested.

The frequency and severity of mitochondrial disease makes it important to develop a range of tools with which to study mitochondrial biology (Park and Larsson, 2011). Our method allows the investigation and comparison of the number, variation and cellular distribution of translationally active mitochondria in normal versus diseased cells, yielding insight into disease aetiology and pathophysiology. Additionally, from a clinical perspective, some classes of important antibiotics cause side effects due to their inhibition of Mt translation resulting from the prokaryotic ancestry of mitochondria (McKee et al., 2006). A simple method of measuring Mt translation would facilitate the screening and monitoring of any side effects of new drugs within this class. Similarly, antiviral ribonucleoside analogues frequently have toxic side effects as mitochondrial RNA polymerase is inhibited (Arnold et al., 2012), and inhibition of mitochondrial transcription would result in reduced Mt translation that, again, could be easily assessed with our method.

In conclusion, protein labelling with HPG in the presence of CHI is a rapid, simple and inexpensive method for the *in-situ* detection of Mt translation with which to investigate the spatial/temporal activity

of mitochondria relative to: (1) other cellular features, (2) in response to internal and external signals, and (3) in relation to normal (e.g. fluctuation of the genome content) and pathological genetic differences.

MATERIALS AND METHODS
Cell culture
C2C12 cells (mouse myoblast), Eph4 cells (mouse spontaneously immortalized mammary epithelium) and MCF-7 cells (human mammary carcinoma) were cultured in Dulbecco's modified Eagle's medium (DMEM, Sigma) with 10% foetal bovine serum, 4.5 g l^{-1} glucose, 110 mg l^{-1} sodium pyruvate, 2 mM L-glutamine, 10 µg ml^{-1} streptomycin and 10 units ml^{-1} penicillin. All cultured cells were routinely tested for contamination with *Mycoplasma spp.* by using the Mycoalert™ kit (Lonza).

Protein labelling
For protein labelling and analysis, cells were grown on Lab-Tek™ II (Nunc), eight-well glass chamber slides until ∼90% confluent. Methionine (Met)-free medium (Sigma) was always supplemented with 2 mM glutamine and 0.0303 mg. mg ml^{-1} cysteine and was used with or without appropriate antibiotics. Immediately prior to labelling, slides were removed from the incubator and placed on a 37°C surface, existing medium was removed and replaced with pre-warmed Met-free medium, this step lasted no more than one minute for any one well. We found no need for the extensive (≥30 min) pre-incubation in Met-free conditions used in previous studies and which were thought necessary for efficient labelling (Beatty et al., 2006; Hodas et al., 2012). Thereafter, the medium was removed and replaced with pre-warmed Met-free medium with or without appropriate antibiotics and with 1 mM homopropargylglycine (HPG) and the slide placed back in the humidified CO_2 incubator for 10 min (or as long as the experiment required).

Cell fixation and click reaction
After that labelling period, slides were immediately placed on ice, medium was removed, washed with ice-cold Buffer A (10 mM HEPES/KOH pH 7.5; 10 mM NaCl; 5 mM $MgCl_2$; 300 mM sucrose). Immediate fixation was with Buffer A supplemented with 3.7% formalin (1/10 dilution from 37% stabilised formaldehyde solution) for 10 min followed by 20 min in PBS with 0.1% Triton X-100. For permeabilising before fixation, the cells were incubated on ice for 2 min in ice-cold buffer A supplemented with 0.015% digitonin. That permeabilising solution was then removed and replaced with Buffer A supplemented with 3.7% formalin (1:10 dilution from 37% stabilised formaldehyde solution) to fix the cells (30 min at room temperature). Cells were then washed several times in PBS. Click reactions were carried out in 100 mM Tris/HCl (pH 8.8), 100 mM ascorbic acid, 1 mM $CuSO_4$ and 10 µM Alexa Fluor® 594 or Alexa Fluor® 488 tagged to azide (Alexa-Fluor-594/488−azide) (Invitrogen or Jena Bioscience, Germany, respectively) for 15 min followed by further washing in PBS. DAPI was used at 0.2 µg ml^{-1} in PBS. In the case (Fig. 4) where the click reaction followed RNA FISH, a different reaction formulation was used to minimise RNA degradation: 40 µM $CuSO_4$, 200 µM BTTAA ligand (Jena Bio, Germany), 10 µM sulpho-cy5 picolyl azide (Picolyl-Azide-Sulfo-Cy5, Jena Bio, Jena, Germany), 5% DMSO, 1 mM ascorbic acid in PBS.

In situ hybridisation
Fixed cells on glass slides were incubated with 0.1 µM Cy3-labelled (single, 5′ terminal conjugate) oligonucleotide (5′-TTACGCCGAAGATAATTAGTT-TGGGTTAATCGTATGACCG-3′) complementary to murine mitochondrial 12S rRNA in 2×SSC, 50% formamide, 10% dextran sulphate, 20 µg ml^{-1} tRNA (*E.coli*) at 60°C for 2 min, then at 40°C for 1 h, followed by removal of unhybridised probe by washing in PBS at 40°C.

Immunofluorescence, antibodies
Fixed cells were incubated in PBS with 0.1% Triton X-100, 2.5% horse serum and an 1:100 dilution of antibody against mitochondrion-encoded cytochrome oxidase 1 [anti-MT-CO1 antibody; Abcam, AB154477 (1D6E1A8), Alexa-Fluor-488 labelled]. Excess antibody was removed by washing with PBS.

Antibiotics and other reagents
Final concentrations of antibiotics used were cycloheximide (CHI; Sigma): 100 µg ml^{-1}; Harringtonine (AbCam): 2 µg ml^{-1}; puromycin (Sigma) 50 µg ml^{-1}; pactamycin (Sigma) 1 µM; chloramphenicol (Sigma) 80 µg ml^{-1}. All antibiotics were added at the same time as HPG, except chloramphenicol which was added to cells 20 min before (and during) incubation with HPG.

Microscopy and image analysis
All images were taken using an epi-fluorescence inverted microscope (Olympus X51, Japan) with a 40× objective lens (Olympus Japan, aperture 0.6 with adjustable focus ring). Total magnification of 400× was obtained by using a digital camera and acquired using the Cell P program at the same exposure time for each fluorophore unless otherwise stated. Images were opened in Image J and those taken with same filters and exposure times were set to identical pixel/intensity threshold settings. Threshold alterations were all linear using the brightness/contrast tool in ImageJ. Lower thresholds were raised only to blacken the space between cells not within cells. Upper thresholds were lowered only make visible any weaker signal towards the edge of cells. Images were coloured by using standard LUTs in Image J. Figures were assembled by using Inkscape and without further intensity manipulation. Colocalisation analysis was carried out individually on 18 cells (entire cell outline) by using Image J with the COL2 plugin to generate the Pearson correlation coefficient. Mean and standard deviation of these measurements were calculated using Excel. For measurement of nucleoid DNA intensity, distinct DAPI staining spots (i.e. not obviously part of cluster) were selected blindly (i.e. without taking translation intensity into account). We excluded those nucleoids close to the nucleus to minimise fluorescence spill-over from nuclear DNA. Once identified, a circle was drawn around the visible local translation that surrounded or was adjacent to the punctate DAPI signal and was designated a region of interest (ROI).

Fluorescence intensity was measured by using Image J: cell areas were selected manually and integrated total fluorescence calculated with the measurement tool. Background signal was measured from eight independent selections in each image and the mean fluorescence determined. Finally, the total corrected cellular fluorescence (TCCF) for each cell was obtained by using TCCF=[integrated fluorescence (density)−(area of selected cell×mean fluorescence of background readings)]. Linear regression and calculation of R^2 were performed using Microsoft Excel.

References
Arnold, J. J., Sharma, S. D., Feng, J. Y., Ray, A. S., Smidansky, E. D., Kireeva, M. L., Cho, A., Perry, J., Vela, J. E., Park, Y. et al. (2012). Sensitivity of mitochondrial transcription and resistance of RNA polymerase II dependent nuclear transcription to antiviral ribonucleosides. *PLoS Pathog* **8**, e1003030.
Beatty, K. E. (2011). Chemical strategies for tagging and imaging the proteome. *Mol. BioSyst.* **7**, 2360-2367.

Beatty, K. E., Liu, J. C., Xie, F., Dieterich, D. C., Schuman, E. M., Wang, Q. and Tirrell, D. A. (2006). Fluorescence visualization of newly synthesized proteins in mammalian cells13. *Angew. Chem. Int. Ed.* **45**, 7364-7367.

Bogenhagen, D. F. (2012). Mitochondrial DNA nucleoid structure. *Biochim. Biophys. Acta* **1819**, 914-920.

Dieterich, D. C., Link, A. J., Graumann, J., Tirrell, D. A. and Schuman, E. M. (2006). Selective identification of newly synthesized proteins in mammalian cells using bioorthogonal noncanonical amino acid tagging (BONCAT). *Proc. Natl. Acad. Sci.* **103**, 9482-9487.

Gao, Y., Bai, X., Zhang, D., Han, C., Yuan, J., Liu, W., Cao, X., Chen, Z., Shangguan, F., Zhu, Z. et al. (2016). Mammalian elongation factor 4 regulates mitochondrial translation essential for spermatogenesis. *Nat. Struct. Mol. Biol.* **23**, 441-449.

Goodman, C. A., Pierre, P. and Hornberger, T. A. (2012). Imaging of protein synthesis with puromycin. *Proc. Natl. Acad. Sci.* **109**, E989.

Gustafsson, C. M., Falkenberg, M. and Larsson, N.-G. (2016). Maintenance and expression of mammalian mitochondrial DNA. *Annu. Rev. Biochem.* **85**, 133-160.

He, Y., Wu, J., Dressman, D. C., Iacobuzio-Donahue, C., Markowitz, S. D., Velculescu, V. E., Diaz, L. A., Jr, Kinzler, K. W., Vogelstein, B. and Papadopoulos, N. (2010). Heteroplasmic mitochondrial DNA mutations in normal and tumour cells. *Nature* **464**, 610-614.

Hodas, J. J. L., Nehring, A., Höche, N., Sweredoski, M. J., Pielot, R., Hess, S., Tirrell, D. A., Dieterich, D. C. and Schuman, E. M. (2012). Dopaminergic modulation of the hippocampal neuropil proteome identified by bioorthogonal noncanonical amino acid tagging (BONCAT). *Proteomics* **12**, 2464-2476.

Konrad, C. G. (1963). Protein synthesis and RNA synthesis during mitosis in animal cells. *J. Cell Biol.* **19**, 267-277.

Kukat, C., Wurm, C. A., Spåhr, H., Falkenberg, M., Larsson, N.-G. and Jakobs, S. (2011). Super-resolution microscopy reveals that mammalian mitochondrial nucleoids have a uniform size and frequently contain a single copy of mtDNA. *Proc. Natl. Acad. Sci.* **108**, 13534-13539.

Larsson, N.-G. (2010). Somatic mitochondrial DNA mutations in mammalian aging. *Annu. Rev. Biochem.* **79**, 683-706.

Mckee, E. E., Ferguson, M., Bentley, A. T. and Marks, T. A. (2006). Inhibition of mammalian mitochondrial protein synthesis by oxazolidinones. *Antimicrob. Agents Chemother.* **50**, 2042-2049.

Pagliarini, D. J., Calvo, S. E., Chang, B., Sheth, S. A., Vafai, S. B., Ong, S.-E., Walford, G. A., Sugiana, C., Boneh, A. and Chen, W. K. (2008). A mitochondrial protein compendium elucidates complex I disease biology. *Cell* **134**, 112-123.

Park, C. B. and Larsson, N.-G. (2011). Mitochondrial DNA mutations in disease and aging. *J. Cell Biol.* **193**, 809-818.

Pestka, S. (1971). Inhibitors of ribosome functions. *Annu. Rev. Microbiol.* **25**, 487-562.

Prescott, D. M. and Bender, M. A. (1962). Synthesis of RNA and protein during mitosis in mammalian tissue culture cells. *Exp. Cell Res.* **26**, 260-268.

Sasarman, F. and Shoubridge, E. A. (2012). Radioactive labeling of mitochondrial translation products in cultured cells. In *Mitochondrial Disorders: Biochemical and Molecular Analysis* (ed. P. D. C. L.-J. WONG), pp. 207-217. Totowa, NJ: Humana Press.

Taylor, R. W., Barron, M. J., Borthwick, G. M., Gospel, A., Chinnery, P. F., Samuels, D. C., Taylor, G. A., Plusa, S. M., Needham, S. J., Greaves, L. C. et al. (2003). Mitochondrial DNA mutations in human colonic crypt stem cells. *J. Clin. Invest.* **112**, 1351-1360.

Uphoff, C. C., Gignac, S. M. and Drexler, H. G. (1992). Mycoplasma contamination in human leukemia cell lines. *J. Immunol. Methods* **149**, 43-53.

Westermann, B. (2010). Mitochondrial fusion and fission in cell life and death. *Nat. Rev. Mol. Cell Biol.* **11**, 872-884.

Wikstrom, J. D., Twig, G. and Shirihai, O. S. (2009). What can mitochondrial heterogeneity tell us about mitochondrial dynamics and autophagy? *Int. J. Biochem. Cell Biol.* **41**, 1914-1927.

Zhang, X., Zuo, X., Yang, B., Li, Z., Xue, Y., Zhou, Y., Huang, J., Zhao, X., Zhou, J., Yan, Y. et al. (2014). MicroRNA directly enhances mitochondrial translation during muscle differentiation. *Cell* **158**, 607-619.